A Method for Wind-Tunnel Investigation of Sonic Booms

Y. S. PAN* AND K. T. WANG†
The University of Tennessee Space Institute, Tullahoma, Tenn.

A theoretical study for a new method for wind-tunnel investigation of sonic boom problem based on large models is presented. Based on the well-known quasi-linear approach, a method for extrapolation of three-dimensional wind-tunnel data obtained in the very near field of an aircraft configuration is obtained. Several numerical examples for axisymmetric and nonaxisymmetric flowfields are given. Comparisons of the present results with those based on the current sonic boom theory show that the three-dimensional near-field effects are important.

I. Introduction

BECAUSE of the development of supersonic transports, the sonic boom problem has been receiving considerable attention in the past decade. Calculations of sonic boom pressure signature of a supersonic aircraft have been based mainly on Whitham's supersonic projectile theory[1] and Hayes and Lomax's supersonic area rule.[2,3] The supersonic area rule shows that the pressure disturbance for a complex three-dimensional configuration can be reduced to the pressure disturbance due to an equivalent body of revolution, provided that the point of interest is sufficiently far from the body. Whitham's theory, on the other hand, describes an asymptotic flow behavior at a distance sufficiently far from a body of revolution. This asymptotic flow obeys the geometric acoustic laws. That is, the flow disturbances are linearly proportional to a local F function which is related to the shape and the flying conditions of the body. The values of the F function are constant along the characteristics emitted from the body. Consequently, the sonic boom pressure signature at a distance sufficiently far from an aircraft can be calculated from the F function of an equivalent body of revolution of the aircraft.

In experimental investigations of the sonic boom in wind tunnels, it is usually necessary to use very small models in order to obtain direct measurements of the far-field pressure signature at the vicinity of a wind tunnel wall (see, for example, Ref. 4). With these small models, inaccuracies with respect to model contours, vibration of model, boundary-layer development, interference of sting supports, small nonuniformities of the free-stream, etc. usually arise. The present method is directed towards an alleviation of this very small model restriction.

The present method is based on large models in wind tunnels, where only the near- or the mid-field is simulated. (Similar methods have also been considered recently.[8]) By measuring the pressure distribution at the vicinity of the wind tunnel wall, it is possible to determine the sonic boom signature at large distances in the outer midfield or in the far field. This method is expected to have great significance in making wind tunnel tests more reliable by avoiding the use of very small models as is usually done today. This method may also have its greatest importance for low fineness ratio and blunt bodies at higher supersonic speeds.

It is well known that, in the near field of an aircraft, the flowfield is fully three-dimensional. The supersonic area rule may not be applied there and hence, Whitham's theory may not be employed directly. Moreover, the flow disturbances in the near field may not be generally described by Whitham's asymptotic relations even within the assumption of the linearized supersonic flow.[5] Indeed, recent wind-tunnel experiments have shown that Whitham's theory does not give good predictions of pressure signature in the near field, especially at large angles of attack.[6] Consequently, the calculation of flow disturbances in a not-so-far-field from an aircraft or the calculation of sonic boom pressure signatures from a known pressure disturbance in a nearer field must be examined.

In the present paper, we shall present a theoretical study of the new wind-tunnel testing method. Particularly, we shall be concerned with the extrapolation of a known pressure signature in the near-field to a distance in the mid- or the farfield. We shall be also concerned with the relationship between the measured pressure signature and the corresponding free-flight pressure signature, both at the vicinity of the wind-tunnel wall.

Following a brief statement of the problem and an outline of the method of analysis (Sec. II), the supersonic flow pattern of a quasi-circular streamtube is considered. A Whitham type F function is defined and then its relations with corresponding flow disturbances are established (Sec. III). The propagation of a known disturbance is treated in Sec. IV. The relationship between the measured pressure signature and the corresponding free flight pressure signature is then obtained in Sec. V. Finally, the new method is summarized, numerical examples are given, and the comparisons with the results based on Whitham's theory and finite-difference approaches are presented and discussed (Sec. VI).

II. Statement of the Problem

A three-dimensional model is tested in a circular cylindrical supersonic wind tunnel with radius R (Fig. 1a). The flow is assumed to be steady, homogeneous, and inviscid. It is well-

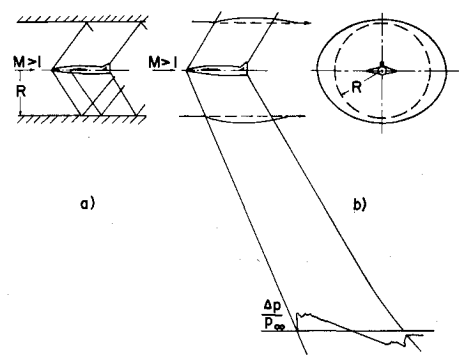

Fig. 1 Flow Patterns of a supersonic aircraft, a) in a wind tunnel, b) enclosed by a streamtube in freeflight.

Presented as Paper 71-184 at the AIAA 9th Aerospace Sciences Meeting, New York, January 25–27, 1971; submitted November 17, 1971; revision received June 22, 1972. This paper is based on research sponsored under the Contract DOT FA 70 WA-2260 by the Federal Aviation Administration whose support is gratefully acknowledged.

Index categories: Supersonic and Hypersonic Flow; Aerodynamic and Powerplant Noise (Including Sonic Boom); Aircraft and Component Wind Tunnel Testing.

* Associate Professor of Aerospace Engineering. Member AIAA.
† Research Assistant. Student Member AIAA.

known that the disturbance emitted from the model is reflected at the wind-tunnel wall, in order that the streamlines adjacent to the wall may be always tangent to the wall. Hence, the pressure disturbance measured at the wind-tunnel wall is not the actual free flight pressure disturbance but the reflected pressure disturbance.

In free flight, however, streamlines may be distorted freely according to the disturbance emitted from the model. Any streamtube enclosing the model of a circular cross section in the free stream may be distorted into a quasi-circular cylindrical shape. Hence, the quantity of flow in the wind tunnel is equal to the quantity of flow confined in a streamtube of the same upstream radius R enclosing this model in free flight (Fig. 1b). Based on the linearized flow theory, the flow disturbance at the distance R in free flight is equal to the incident disturbance on the wind-tunnel wall.

Inside the wind tunnel, if the flowfield over the tested model can be described by the linearized supersonic flow theory, and if the cumulative nonlinear effects can be neglected within the wind tunnel, then the flowfield near the wall may also be described by the linearized supersonic equations. It is possible to relate the reflected disturbance with the incident disturbance at the wall by specifying proper wall boundary conditions.

In free flight, it is known that the flow disturbance outside the streamtube of upstream radius R due to the presence of the model is equivalent to that caused by this streamtube or by any other streamtubes enclosing this model in nearer fields. The shape of the streamtube of upstream radius R, which is usually represented by a superposition of various multipole distributions in the linearized theory, may be obtained in terms of the known disturbance at R. By defining a Whitham type F function in terms of these distributions, one obtains the F function for this streamtube of upstream radius R, which can be related to the flow disturbances at R.

The propagation of a known F function from one streamtube to another one further afield may be treated based on Whitham's hypothesis on the improvement of characteristics. That is, the values of F function are constant along bicharacteristics in the three-dimensional flow. Thus the new F function may be obtained for any streamtube further afield. However, it may generally have multiple values in certain regions of its arguments; these are due to the intersection of characteristic surfaces in the physical space where values of physical quantities cease to be unique. This failure of the linearized supersonic theory as a description of the flow is known to be remedied by the presence of shock surfaces. The positions of shock surfaces may be determined by the usual simple geometric property; namely, to the first order of the shock strength, the shock surface bisects the angle between the two intersecting characteristic surfaces. Having fixed the positions of shocks, the new F function becomes a single valued function, which actually is the Whitham type local F function of the corresponding streamtube further afield. Finally, from the new single valued F function, the flow disturbances may be obtained.

III. F Function and Its Relationship to the Flow Disturbances

As stated in Sec. II, to consider a supersonic flowfield downstream of a three-dimensional complex body, we may study the flowfield downstream of a streamtube enclosing this body. If the flow disturbance is weak on the surface of the streamtube, this streamtube is generally of a quasi-cylindrical shape and the flow over it may be described by the linearized supersonic flow theory. In this section, we shall consider a supersonic flow over an arbitrary quasi-cylindrical streamtube with upstream radius R enclosing the body (R will be identified as the radius of the wind tunnel in Sec. IV and V).

Let us choose the body axis to be the x axis coinciding with the freestream direction (Fig. 2). Enclosing this body we choose a co axial quasi-cylindrical streamtube with an arbitrary upstream radius R ($R = 0$ corresponds to a point-nosed slender body). On the surface of this streamtube, the flow is assumed to be disturbed at $x = 0$ where the origin of the x axis is located. The r axis perpendicular to the x axis is the radial coordinate and θ is the polar coordinate measured counter-clockwisely from the vertically downward r-direction. We further assume that the entire problem is symmetric with respect to $\theta = 0$ (or π) plane.

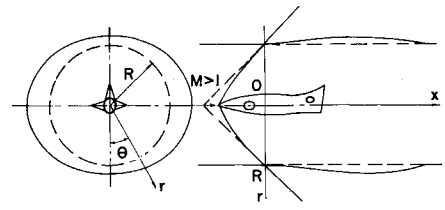

Fig. 2 Quasi-circular streamtube and coordinate system.

Let the freestream velocity and Mach number be U and M, respectively, and at a general point (x, r, θ) the local velocity be $(U + Uu, Uv, Uw)$. The flow is assumed to be irrotational; hence the velocity disturbances u, v and w may be deduced from a velocity potential φ. On the linearized theory, φ satisfies the equation

$$\partial^2\varphi/\partial r^2 + (1/r)(\partial\varphi/dr) + (1/r^2)(\partial^2\varphi/\partial\theta^2) - \beta^2(\partial^2\varphi/\partial x^2) = 0 \quad (1)$$

where $\beta^2 = M^2 - 1$. A general solution of Eq. (1) which represents a disturbance propagating downstream from the quasi-cylinder is[7]

$$\varphi = -\sum_n \cos n\theta \int_{-\alpha R}^{x-\alpha r} \frac{h_n[(x-t)/\beta r] f_n(t)\, dt}{[(x-t)^2 - \beta^2 r^2]^{1/2}} \quad (2)$$

Here, $h_n(t) = \cosh[n \cosh^{-1} t]$; $f_n(t)$ are the multipole distributions and may be related to the shape of the quasi-cylindrical streamtube. Disturbance velocity components can be deduced from Eq. (2) by differentiations; for example

$$u = -\sum_n \cos n\theta \int_{-\alpha R}^{x-\alpha r} \frac{h_n[(x-t)/\beta r] f_n'(t)\, dt}{[(x-t)^2 - \beta^2 r^2]^{1/2}} \quad (3)$$

The pressure disturbance relates to the velocity disturbance by the linearized Bernoulli's equation

$$P \equiv \Delta p/\rho_\infty U^2 = (p - p_\infty)/\rho_\infty U^2 = -u \quad (4)$$

In the far field, by changing the integration variable, replacing $x - \beta r$ by $y - \beta R$ in Eq. (3) and making a farfield approximation, $\beta r/y \gg 1$, the expression for u written in the Fourier series expansion, reduces to

$$u = \sum_n u_n \cos n\theta = -\frac{1}{(2\beta r)^{1/2}} \sum_n F_n(y) \cos n\theta \quad (5)$$

Similarly,

$$v = \sum_n v_n \cos n\theta = \frac{\beta}{(2\beta r)^{1/2}} \sum_n F_n(y) \cos n\theta \quad (6)$$

$$w = \sum_n w_n \sin n\theta = \frac{1}{r(2\beta r)^{1/2}} \sum_n n\, G_n(y) \sin n\theta \quad (7)$$

Here, y is the characteristic parameter of a linearized characteristic curve $[x - \beta(r - R) = y]$ on $\theta =$ constant plane

$$F_n(y) = \int_0^y \frac{f_n'(t - \beta R)\, dt}{(y-t)^{1/2}} \quad (8)$$

being the Fourier components of the Whitham type F function of the streamtube

$$F(y, \theta) = \sum_n F_n(y) \cos n\theta \quad (9)$$

and

$$G_n(y) = \int_0^y \frac{f_n(t - \beta R)\, dt}{(y-t)^{1/2}} = \int_0^y F_n(t)\, dt \quad (10)$$

It may be noted that, for bodies of revolution ($n = 0$), the above relations are the asymptotic linear relations of Whitham[1];

for bodies of revolution at small angles of attack ($n = 0$ and 1), the relations reduce to those of Siegelman.[9] It may also be pointed out that, in the above relations, u and v vary as $r^{-1/2}$ and w varies as $r^{-3/2}$; hence, in the far field, w may be neglected in comparison with u or v. Consequently u, v and P may be related directly to the F function of an equivalent body of revolution. This is the basis on which the current sonic boom calculations are made.

In a not-so-far field, it has been shown[5] that it is possible, within the linearized supersonic flow theory, to obtain exact relations between the flow disturbances and the corresponding local F function on a streamtube enclosing an axisymmetric body. Now we shall obtain the similar relations at R for the nonaxisymmetric flow. Observe that Eq. (8) is an Abel integral equation whose solution is

$$f_n'(t - \beta R) = \frac{1}{\pi}\frac{d}{dt}\int_0^t \frac{F_n(x)\,dx}{(t-x)^{1/2}} = \frac{1}{\pi}\int_0^t \frac{F_n'(x)\,dx}{(t-x)^{1/2}} \tag{11}$$

since $F_n(0) = 0$. If Eq. (11) is substituted into the solution of the flow disturbances, for example Eq. (3) at R noting Eq. (4) and the form indicated in Eq. (5), we obtain

$$\begin{Bmatrix} P_n(x) \\ -u_n(x) \end{Bmatrix} = \frac{1}{(2\beta R)^{1/2}}\int_0^x F_n'(t)\,K_n\left(\frac{x-t}{\beta R}\right)dt \tag{12}$$

where

$$K_n(x) = \frac{2^{3/2}}{\pi}\int_0^{\pi/2} \frac{h_n(x\cos^2\phi + 1)\,d\phi}{(2 + x\cos^2\phi)^{1/2}} \tag{13}$$

Noting that $K_n(0) = 1$, we integrate Eq. (12) by parts to obtain

$$\begin{Bmatrix} P_n(x) \\ -u_n(x) \end{Bmatrix} = \frac{1}{(2\beta R)^{1/2}}\left[F_n(x) + \frac{1}{\beta R}\int_0^x F_n(t)K_n'\left(\frac{x-t}{\beta R}\right)\right] \tag{14}$$

Similarly, we may obtain the relations of v_n and w_n in terms of F_n and G_n, respectively

$$v_n(x) = \frac{\beta}{(2\beta R)^{1/2}}\left[F_n(x) + \frac{1}{\beta R}\int_0^x F_n(t)J_n'\left(\frac{x-t}{\beta R}\right)dt\right] \tag{15}$$

$$w_n(x) = \frac{n}{R(2\beta R)^{1/2}}\left[G_n(x) + \frac{1}{\beta R}\int_0^x G_n(x)K_n'\left(\frac{x-t}{\beta R}\right)dt\right] \tag{16}$$

where

$$J_n(x) = \frac{2^{3/2}}{\pi}\int_0^{\pi/2} \frac{(x\cos^2\phi + 1)h_n(x\cos^2\phi + 1)\,d\phi}{(2 + x\cos^2\phi)^{1/2}} \tag{17}$$

Since Eqs. (14–16) are the integral equation of the second kind, we may solve for F_n and G_n in terms of the Fourier components of flow disturbances at R

$$\frac{F_n(x)}{(2\beta R)^{1/2}} = \begin{Bmatrix} P_n(x) \\ -u_n(x) \end{Bmatrix} - \frac{1}{\beta R}\int_0^x \begin{Bmatrix} P_n(t) \\ -u_n(t) \end{Bmatrix} S_n\left(\frac{x-t}{\beta R}\right)dt \tag{18}$$

$$\frac{\beta F_n(x)}{(2\beta R)^{1/2}} = v_n(x) - \frac{1}{\beta R}\int_0^x v_n(t)\,T_n\left(\frac{x-t}{\beta R}\right)dt \tag{19}$$

$$\frac{nG_n(x)}{R(2\beta R)^{1/2}} = w_n(x) - \frac{1}{\beta R}\int_0^x w_n(t)\,S_n\left(\frac{x-t}{\beta R}\right)dt \tag{20}$$

Here, S_n and T_n are resolvent kernels of K_n' and J_n', respectively. K_n' J_n' are the differentiations of K_n and J_n, respectively, with respect to their arguments. Some S_n, T_n, K_n' and J_n' have been computed and tabulated in Ref. 10. (S_0, T_0, K_0' and J_0' were denoted, respectively, as S, S_1, K' and K_1' in Ref. 5.)

Since the streamtube of upstream radius R was chosen arbitarily, the relationship between the flow disturbances and F_n or G_n [Eqs. (14–16) or Eqs. (18–20)] is valid for any R within the linearized supersonic flow theory. As $R \to \infty$, these relations reduce to the asymptotic linear relations Eqs. (5–7). The second terms in Eqs. (14–16) and Eqs. (18–20) represent the corrections of the asymptotic relations in a nearer field.

IV. Propagation of the Flow Disturbances

Since the relations, Eqs. (14–16), are valid at any distance where the flow disturbances are weak, we may now write the expressions for flow disturbances at any distance r from the axis in terms of the corresponding local F function,

$$\begin{matrix} \frac{1}{\gamma M^2}\frac{\Delta p}{p_\infty} \\ -u \end{matrix} = \frac{1}{(2\beta r)^{1/2}}\left[F(y,\theta_0) + \frac{1}{\beta r}\sum_n \cos n\theta_0 \int_0^y F_n(t)K_n'\left(\frac{y-t}{\beta r}\right)dt\right] \tag{21}$$

$$v = \frac{\beta}{(2\beta r)^{1/2}}\left[F(y,\theta_0) + \frac{1}{\beta r}\sum_n \cos n\theta_0 \int_0^y F_n(t)\,J_n'\left(\frac{y-t}{\beta r}\right)dt\right] \tag{22}$$

$$w = \frac{-1}{r(2\beta r)^{1/2}}\frac{\partial}{\partial\theta_0}\left[\sum_n G_n(y)\cos n\theta_0 + \frac{1}{\beta r}\sum_n \cos n\theta_0 \int_0^y G_n(t)K_n'\left(\frac{y-t}{\beta r}\right)\right] \tag{23}$$

Here, $y = x - \beta(r - R) = \text{const}$ is a linear characteristic (straight) line on a plane with azimuth angle $\theta_0 = \text{const}$; on the mean surface of the streamtube representing the wind tunnel, $r = R$, $y = x$. As $F(y, \theta_0) = \text{const}$ along linear characteristic lines, $y = \text{const}$, on planes with aximuth angle $\theta_0 = \text{const}$, Eqs. (21–23) represent the solution of flow disturbances in the classical linearized theory.

It has long been recognized that the linearized solution is not uniformly valid to the far field due to the so-called cumulative nonlinear effects.[16] In the development of the supersonic projectile theory, Whitham[1] made the hypothesis that linearized theory gives a correct first approximation everywhere, provided that the value which it predicts for any physical quantity on the approximate (linear) characteristic from a given point on the axis is interpreted as the value, at the same distance from the axis, on the exact characteristic (improved to the first-order velocity disturbances) from the same point. Now we shall apply the same hypothesis to the present three-dimensional problem.

In three-dimensional supersonic flows, two-dimensional characteristic curves on constant-azimuth-angle planes are replaced by bicharacteristic curves in a three-dimensional space. Bicharacteristic curves are tangential lines common to the characteristic surfaces and to the characteristic conoids (for detailed discussion, see Hayes and Probstein[11]). For the present problem of the linearized supersonic flow, the characteristic surfaces are surfaces of revolution with respect to the body axis.[12] Through a general point (x, r, θ) on a characteristic surface, the bicharacteristic direction may be found from the tangential direction common to the characteristic surface and to the local Mach cone

$$\frac{\Delta x}{\Delta r} = \frac{(q^2 - v^2)^{1/2}(1+u)\cos\mu - (1+u)v\sin\mu}{(q^2 - v^2)^{1/2}v\cos\mu + (q^2 - v^2)\sin\mu}$$

$$\frac{r\Delta\theta}{\Delta r} = w\frac{(q^2 - v^2)^{1/2}\cos\mu - v\sin\mu}{(q^2 - v^2)^{1/2}v\cos\mu + (q^2 - v^2)\sin\mu}$$

with μ and q being the local Mach angle and the local nondimensional velocity, respectively. By using the definitions of μ and of q and by neglecting the second and higher order terms of flow disturbances, we obtain the differential equations of the bicharacteristics to the first-order velocity disturbances,

$$\partial x/\partial r = \beta + [(\gamma + 1)M^4/2\beta]u - M^2(v + \beta u) \tag{24}$$

$$\partial\theta/\partial r = \beta w/r \tag{25}$$

To obtain a set of parametric equations of the bicharacteristics, we may substitute Eqs. (21) and (22) into Eqs. (24) and (25) and perform integrations along the line $y = \text{constant}$ and $\theta_0 = \text{constant}$

$$x = \beta(r - R) + y - kF(y,\theta_0)(r^{1/2} - R^{1/2}) - \int_R^r L(y,\theta_0,r)\,dr \tag{26}$$

and

$$\theta = \theta_0 + \int_R^r \frac{\beta w}{r}\,dr, \tag{27}$$

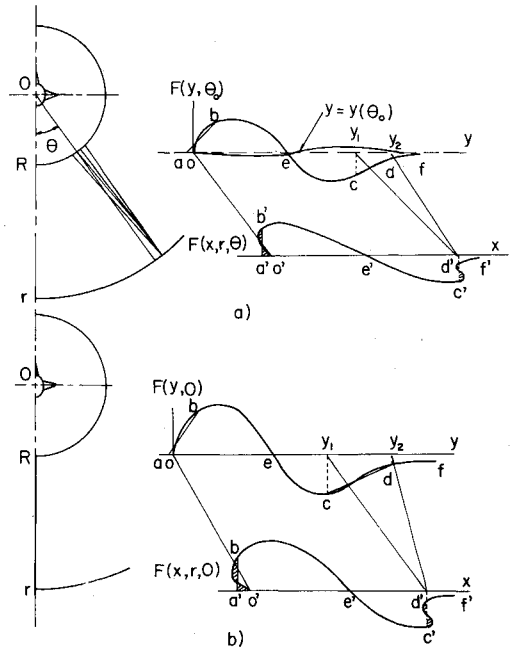

Fig. 3 Propagation and distortion of F functions; a) $F(y, \theta_0)$, b) $F(y, 0)$.

with $$k = 2^{-1/2}(\gamma + 1)M^4\beta^{-3/2} \tag{28}$$

and $$L = \frac{(\gamma+1)M^4}{\beta(2\beta r)^{3/2}} \sum_n \cos n\theta_0 \int_0^y F_n(t) K_n'\left(\frac{y-t}{\beta r}\right) dt + M^2(v + \beta u) \tag{29}$$

Here, γ and θ_0 are the coordinates x and θ, respectively, of a point on the streamtube of the wind-tunnel with a mean surface of radius R. y = constant and θ_0 = constant in Eqs. (26) and (27), respectively, define a bicharacteristic curve from the said point ($r = R$, $x = y$, $\theta = \theta_0$). Based on Whitham's hypothesis, as $F(y, \theta_0)$ = constant along the bicharacteristic curves, y = const and θ_0 = const, defined by Eqs. (26) and (27); Eqs. (21–23) represent a first approximate solution of flow disturbances valid everywhere in the three-dimensional flowfield. It is worth while to note that, for an axisymmetric flowfield ($n = 0$), $w = 0$ and $\theta = \theta_0$ = const, Eqs. (24, and 25) reduce to Whitham's characteristic differential equation,[1] and Eq. (26) reduces to the improved characteristic equation obtained by Pan.

Once $F(y, \theta_0)$ is known at R, we may integrate Eqs. (26) and (27) to obtain $F(x, r, \theta)$ at any cylindrical surface further afield at r. The value of F at a particular point (x, θ) at r is equal to the value of $F(y, \theta_0)$ at a point (y, θ_0) which is on the same bicharacteristic curve as the point (x, θ) at r. Because of the θ-component disturbance, the bicharacteristic curve from (y, θ_0) is generally not lying on the same θ_0 plane (see Fig. 3a). The bicharacteristics which pass through a straight line θ = const on the surface r originate on the surface at R from a curve $\theta_0 = \theta_0(y)$. Consequently, to determine $F(x, r, \theta)$ on a line θ = const at r, we have to determine the curve $\theta_0 = \theta_0(y)$ at R. On the plane of symmetry $\theta = 0$ (or π) where $w = 0$, all bicharacteristic curves remain in the same plane; hence, $F(x, r, 0)$ is determined only by $F(y, 0)$ at R (Fig. 3b). The shape of the F function obtained at r is generally distorted and different from the original F function at R. The F function on an θ = const line at r is generally a multivalued function of its argument x. The multivalued regions are due to the intersection of characteristic surfaces in the physical space where values of physical quantities cease to be unique. This failure of the linear theory as a description of the flow is known to be remedied by the presence of shock surfaces.[13]

It is well known[13] that the shocks, to a first-order in strength, can be determined by a simple geometric property, that is, a shock surface bisects the angle between two intersecting characteristic surfaces. As shown by Whitham[1] the F function, at least in the far field, gives a rough description of the flow pattern, since it shows whether the characteristics are converging in compression where a shock will appear, or diverging in expansion. The shock position at any distance r may be determined from the F function at R. For axisymmetric flows, Whitham obtained a relation called "area-balance-rule" which states that the lobes cut off on each side of the F function by a straight segment which determines a shock position must be equal in the area. The slope of the straight segment depends on the distance r. Following Whitham's procedure we can obtain general relations for determining shock positions.

Suppose that a general shock surface intersects θ = const at r at a point

$$x = \beta(r - R) - G(r, \theta) \tag{30}$$

At the point (r, x, θ) the shock surface intersects two bicharacteristics, specified by y_1 and y_2 ($y_2 > y_1$) on $\theta_0 = \theta_0(y)$ at R, in two corresponding characteristic surfaces (see points c and d in Fig. 3). The bisection of the angle between the characteristic surfaces by the shock surface requires that, projecting on the θ = const plane

$$2\frac{\partial G}{\partial r} = \tfrac{1}{2}k r^{-1/2}\{F[y_1, \theta_0(y_1)] + F[y_2, \theta_0(y_2)]\} + \{L[y_1, \theta_0(y_1); r] + L[y_2, \theta_0(y_2); r]\} \tag{31}$$

On the other hand, elimination of $x - \beta(r - R)$ from the Eqs. (30) and (26) for y_1 and y_2 gives, respectively,

$$G(r, \theta) = kF[y_1, \theta_0(y_1)][r^{1/2} - R^{1/2}] + \int_R^r L[y_1, \theta_0(y_1); r]\, dr - y_1 \tag{32}$$

$$G(r, \theta) = kF[y_2, \theta_0(y_2)][r^{1/2} - R^{1/2}] + \int_R^r L[y_2, \theta_0(y_2); r]\, dr - y_2 \tag{33}$$

G and r as functions of y_1 and y_2 can be solved from Eqs. (31–33) and then the relation between y_1 and y_2 is obtained.

The relation between r and y_1 (and/or y_2) is obtained by eliminating G from Eqs. (32) and (33).

$$\frac{F[y_2, \theta_0(y_2)] - F[y_1, \theta_0(y_1)]}{y_2 - y_1} = \left\{ K(r^{1/2} - R^{1/2}) + \frac{\int_R^r \{L[y_2, \theta_0(y_2); r] - L[y_1, \theta_0(y_1); r]\} dr}{F[y_2, \theta_0(y_2)] - F[y_1, \theta_0(y_1)]} \right\}^{-1} \tag{34}$$

For large r, Eq. (34) reduces to a relation obtained by Whitham,[1] for $R = 0$

$$\frac{F[y_2, \theta_0(y_2)] - F[y_1, \theta_0(y_1)]}{y_2 - y_1} = \frac{1}{k(r^{1/2} - R^{1/2})} \tag{35}$$

The geometric interpretation of Eq. (35) is that the slope of the straight segment adjoining the points y_1 and y_2 of the F function curve at R relates to r only. For an arbitrary r, the slope of segment cd relates not only to r but to y_1, y_2 and F. For different shocks, the slopes of the corresponding segments are different.

If Eqs. (32) and (33) are differentiated with respect to r and added, and then the term $2\,\partial G/\partial r$ is replaced by Eq. (31), the equation

$$\begin{aligned}[k(r^{1/2} - R^{1/2})\, F'(y_1, \theta_0(y_1)) - 1]\, dy_1 \\ + [k(r^{1/2} - R^{1/2})\, F'\{y_2, \theta_0(y_2)\} - 1]\, dy_2 \\ = -[dy_1 \frac{\partial}{\partial y_1}\int_R^r L\{y_1, \theta_0(y_1); r\}\, dr \\ + dy_2 \frac{\partial}{\partial y_2}\int_R^r L\{y_2, \theta(y_2); r\}\, dr]\end{aligned} \tag{36}$$

is obtained. By eliminating $k(r^{1/2} - R^{1/2})$ from Eqs. (34) and (36) and with some manipulation, we obtain the relation between y_1 and y_2 or the position of cd on the F function curve at R;

$$\int_{y_1}^{y_2} F[y\, \theta_0(y)]\, dy = \tfrac{1}{2}(y_2 - y_1)\{F[y_1, \theta_0(y_1)] + F[y_2, \theta_0(y_2)]\}$$

$$+\tfrac{1}{2}\{F[y_1,\theta_0(y_1)]+FF[y_2,\theta_0(y_2)]\}$$
$$\int_R^r\{L[y_1,\theta_0(y_1);r]-L[y_2,\theta_0(y_2);r]\}\,dr \tag{37}$$
$$+\int_{y_1}^{y_2}F[y,\theta_0(y)]\,dy\,\frac{\partial}{\partial y}\int_R^r L[y,\theta_0(y);r]\,dr$$

The preceding equation replaces the well-known "area-balance-rule" (Ref. 1)

$$\int_{y_1}^{y_2}F[y,\theta_0(y)]dy=\tfrac{1}{2}(y_2-y_1)\{F[y_1,\theta_0(y_1)]+F[y_2,\theta_0(y_2)]\} \tag{38}$$

Now Eq. (37) together with Eq. (34) determines the positions of y_1 and y_2 on $F(y,\theta_0(y))$ for a fixed r. These relations may also be used to determine the positions of other shocks; for example, the position of the front shock ab (Fig. 3) may be determined by setting $F[y_1,\theta_0(y_1)]\equiv 0$ at the point a on the F function curve. We may note that Eqs. (34) and (37) are so complex that no explicit solution for $r(y_1,y_2)$ is possible. Results may only be obtained by a numerical iterative procedure by using Eqs. (35) and (38) as a first approximation.

After having determined the positions of shocks, the local F function at r becomes a single valued function except with a finite number of discontinuities. The corresponding flow disturbances may be determined from the local F function and its Fourier components by Eqs. (21–23) or Eqs. (14–16) by replacing R by r.

V. Wind-Tunnel Wall Reflection

In this section, we shall obtain the relation between the free flight (incident) pressure disturbance and the measured (reflected) pressure disturbance at the cylindrical wind tunnel wall. We assume that the flow in the wind tunnel may be described by the linearized supersonic flow theory. The pressure (Mach) waves generated by the model propagated outward and downstream are reflected at the wind-tunnel wall; the reflected waves will not interact with the model. Unlike the reflection of a plane wave from a rigid plane surface which gives a constant reflection factor 2.0, the reflection of a curved wave from a cylindrical rigid surface may not be described by a simple constant reflection factor. Since the flowfield behind a curved wave is generally not uniform, the flowfield behind a curved reflected wave depends on both the incident curved wave and the distance from the wave front.

Referring to Fig. 1a with the coordinates described in Fig. 2, the disturbance velocity potential φ in the wind tunnel satisfies Eq. (1). Equation (1) together with the uniform freestream boundary conditions may be solved by a technique of Laplace transform, i.e.

$$\bar{\varphi}(s,r,\theta)=\frac{1}{\beta R}\int_0^\infty\varphi(x,r,\theta)\,e^{-sx/\beta R}dx \tag{39}$$

The general solution to the transformed governing equation (1) is given by[7]

$$\bar{\varphi}(s,r,\theta)=\sum_n\cos n\theta\,A_nK_n(sr/R)\left[1-\frac{K_n'(s)\,I_n'(sr/R)}{I_n'(s)\,K_n'(sr/R)}\right] \tag{40}$$

where the boundary condition on the rigid wall ($\partial\varphi/\partial r=0$ at $r=R$) has been satisfied. K_n and I_n are the modified Bessel functions and A_n is a function of s only. [Readers should not be confused by K_n in this section with the K_n defined by Eq. (13) in Sect. III].

The transformed disturbance pressure $\bar{P}$ is, by Eqs. (4) and (39),

$$\bar{P}(s,r,\theta)=-(s/\beta R)\,\bar{\varphi}(s,r,\theta) \tag{41}$$

On the wind-tunnel wall ($r=R$), the disturbance pressure is the measured (reflected) pressure and is denoted by $\bar{P}_R$

$$\bar{P}_R(s,R,\theta)=\sum_n\cos n\theta\,\bar{P}_{Rn}(s,R) \tag{42}$$

with $\bar{P}_{Rn}$ being the Fourier components of $\bar{P}_R$; from Eqs. (40) and (41)

$$\bar{P}_{Rn}(s,R)=-(s/\beta R)A_nK_n(s)\{1-[K_n'(s)\,I_n(s)/I_n'(s)\,K_n(s)]\} \tag{43}$$

On the other hand, it is easy to show that the Fourier components of the free-flight (incident) disturbance pressure on the wall is

$$\bar{P}_{In}(s,R)=-(s/\beta R)\,A_nK_n(s) \tag{44}$$

Hence, by combining Eqs. (43) and (44), we may express the free-flight pressure in terms of the measured pressure

$$\bar{P}_{In}(s,r)=\tfrac{1}{2}\bar{P}_{Rn}(s,R)\,sK_n(s)[I_{n+1}(s)+I_{n-1}(s)] \tag{45}$$

Now the relations between $P_{In}(x,R)$ and $P_{Rn}(x,R)$ may be obtained by performing the inverse Laplace transform

$$P_{In}(x,R)=\tfrac{1}{2}\,P_{Rn}(x,R)-\frac{1}{\beta R}\int_0^x P_{Rn}(t,R)R_n\left(\frac{x-t}{\beta R}\right)dt\ ,\quad x>0$$
$$=0\qquad x<0 \tag{46}$$

Here, $R_n(x)$, the reflection functions, are the inverse Laplace transform of $\bar{R}_n(s)$

$$\bar{R}_n(s)=1-s\,K_n(s)[I_{n+1}(s)+I_{n-1}(s)] \tag{47}$$

Since the Laplace inversing of the $\bar{R}_n(s)$ is not known at the present, exact values of $R_n(x)$ for all n and x can not be obtained. However, for most practical cases, the argument of $R_n(x)$ is usually small, and we may obtain an asymptotic expression of $R_n(x)$ for small x by inverting the asymptotic expression of $\bar{R}_n(s)$ for large s. The result is

$$R_n(x)=\sum_{m=1}C_{nm}\,x^{m-1}/8^m(m-1)! \tag{48}$$

where

$$C_{nm}=\sum_{\substack{i=0\\ i+j=m}}^{m}(-1)^j\,a_{ni}b_{nj}$$

with

$$a_{ni}=\prod_{j=1}^{i}\frac{4n^2-(2j-1)^2}{j}$$

$$b_{ni}=\tfrac{1}{2}\left\{\prod_{j=1}^{i}\left[\frac{4(n+1)^2-(2j-1)^2}{j}\right]+\prod_{j=1}^{i}\left[\frac{4(n-1)^2-(2j-1)^2}{j}\right]\right\}$$

and $a_{n0}=b_{n0}=1$. After having obtained $P_{In}(x,R)$, we may sum $P_{In}\cos n\theta$ to obtain the corresponding free-flight pressure disturbance $P_I(x,R,\theta)$ at the wind-tunnel wall.

VI. Summary of the Method and Examples

In this section, the present method and its procedures of calculation are summarized. Several typical examples based on the present analysis are presented and compared with the results based on other methods.

A three-dimensional pressure disturbance $P_R(x,\theta,R)$ is measured at a circular cylindrical wind tunnel of radius R (for example, by using a scanning system suggested by R. C. Bauer of ARO, Inc. to the senior author[14]). This three-dimensional disturbance is expanded in the Fourier series in θ; then the Fourier components $P_{Rn}(x,R)$ can be obtained. By using the relations, Eq. (46), the corresponding Fourier components $P_{In}(x,R)$ of the incident (free flight) pressure disturbance $P_I(x,\theta,R)$ and then $P_I(x,\theta,R)$ can be found. $P_I(x,\theta,R)$ is the three-dimensional disturbance on a streamtube with upstream radius R which corresponds to the wind tunnel in free flight. (At present, the incident pressure measurements are normally made by some type of static pressure probe at a fixed position outside of the wall boundary layer. Signatures for a variety of aximuth angles are obtained by rolling the model).

By using the pressure disturbance $P_I(x,\theta,R)$ or $P_{In}(x,R)$, we can calculate the local $F(y,\theta_0,R)$ function of this streamtube from Eqs. (14) and (21). $F(y,\theta_0,R)$ represents the disturbance

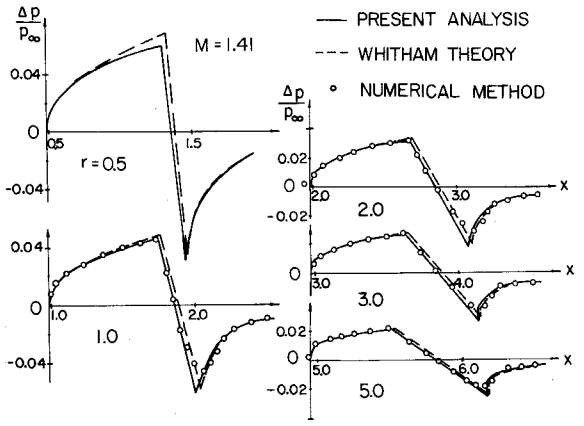

Fig. 4 Near-field pressure signatures (M = 1.41).

generated by the streamtube with upstream radius R or by the tested model in the free flight and propagates to a distance r in further afield along bicharacteristics given by Eqs. (26) and (27). Having fixed shock positions on the $F(y, \theta_0, R)$ curve by Eqs. (34) and (37), the new single valued local $F(x, r, \theta)$ function is obtained at r. This new F function is then expanded in the Fourier series. Corresponding to Fourier components $F_n(x, r)$, the Fourier components of pressure disturbance $P_n(x, r)$ are found from Eq. (14). Finally, the three-dimensional pressure disturbance $P(x, \theta, r)$ is obtained by summing up all Fourier components.

Several numerical calculations of near-field pressure signatures were performed. The streamwise positions of the experimental data with respect to the models are usually not given. Furthermore, no complete three-dimensional experimental data at a constant distance from a model are available. Therefore, a quantitative comparison of the present analysis with experimental data is not possible at present. Thus, we shall only present the comparisons of the present analysis with other theoretical calculations. Typical examples are presented and discussed in the following.

Figure 4 shows the near-field pressure signatures at $r = 0.5$, 1.0, 2.0, 3.0, and 5.0 from the axis of a 6.46° half-angle cone-cylinder body. The length l of the cone portion is taken to be 1.0; the freestream Mach number is 1.41. Comparisons show the differences between the signatures of the present analysis and of the Whitham theory. The differences are due to the present correction of the linear asymptotic relations between the flow disturbances and the local F function and due to the shifts of the characteristic curves (the shifts are as large as 20% of Whitham's value at $r = 0.5$). The peak pressures predicted by the present analysis are generally lower than and located ahead of those predicted by the Whitham theory especially at tail shocks. This prediction is qualitatively consistent with some of the near-field experimental observations (for example, Ref. 6).

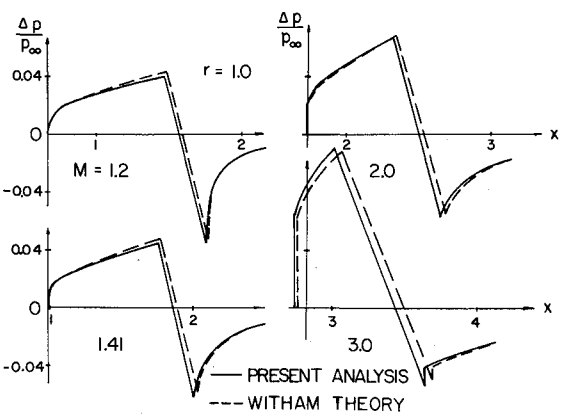

Fig. 5 Near-field pressure signatures (R = 1.0).

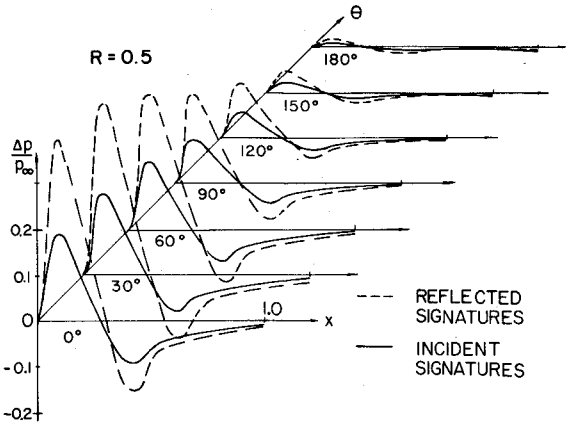

Fig. 6 Reflected and incident three-dimensional signature at the wind-tunnel wall.

In Fig. 4, numerical pressure data are also presented. These data were obtained by Kutler ‡ using a shock-capturing finite-difference approach.[15] The present signatures are generally in excellent agreement with the numerical results except at the neighborhood of the shock waves. The difference near the shock waves is due to the fact that, in the shock-capturing finite-difference approach, the shock waves which occur will spread over a few mesh intervals. Hence, the exact positions of the shock waves can not be exactly predicted by this numerical method.

Figure 5 shows the comparison of pressure signatures based on the present analysis and the Whitham theory at $r = 1.0$ of the same cone-cylinder body at several different Mach numbers. Because of the larger shifts of characteristics at larger Mach numbers, larger shifts of pressure signatures appear.

Figures 6 and 7 demonstrate an extrapolation of a measured three-dimensional signature. A three-dimensional measured (reflected) pressure signature is assumed in a form $P_R = P_{R0} + P_{R1} \cos\theta$ and is shown in the dashed lines in Fig. 6. A freestream Mach number of $M = 2.0$ and a wind-tunnel wall radius of $R = 0.5$ are assumed. The corresponding incident (free flight) signature is calculated and shown in the solid lines in Fig. 6.

Following the procedures summarized above, the extrapolated pressure signatures at $r = 10.0$ are shown in the solid lines in Fig. 7. These signatures near the leading shock waves are fixed approximately from the 13-term Fourier representation of the pressure signatures which are shown in the dotted lines. The pressure signatures obtained by a simple extrapolation based on the current sonic boom theory are also shown in the dashed lines. For this example, the current sonic boom theory over-

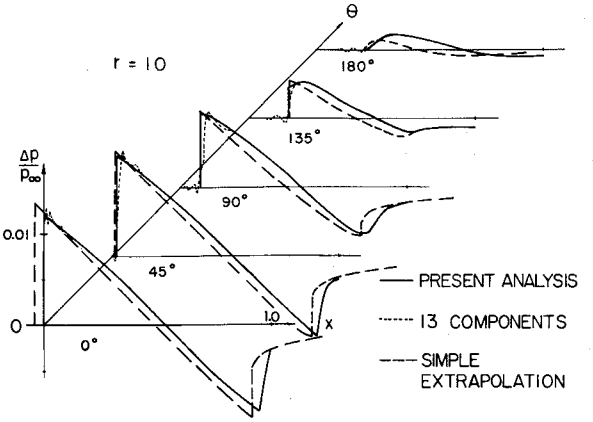

Fig. 7 Comparisons of pressure signatures.

‡ Numerical data generously provided by P. Kutler of NASA Ames Research Center are gratefully acknowledged.

estimates the peak over pressure for $0 \leqq \theta \leqq 90°$ as much as 10%, but it under estimates the peak overpressures for $90° \leqq \theta \leqq 180°$ as much as 40%. Although no general quantitative conclusion on the importance of the near field effects can be obtained from this single example, this example does show that the near-field effects may be important for extrapolating complex near-field three-dimensional signatures.

VII. Concluding Remarks

A theoretical study for a new method for wind-tunnel investigations of the sonic boom problem based on large models is presented. Based on the linearized supersonic flow theory, the corresponding free-flight pressure disturbance at the distance of the wind-tunnel wall may be calculated from the measured pressure disturbance at the wind-tunnel wall, and the flow disturbances can be written in terms of a local Whitham's type F function. Based on Whitham's hypothesis on the improvement of the linear theory, the F function propagates to the downstream along bicharacteristic curves. Near-field and three-dimensional effects are considered in the analysis. Several numerical examples are presented. Comparisons of the present results with those based on the current sonic boom theory and a numerical method are discussed. More near-field experimental measurements using axisymmetric and three-dimensional bodies and more calculations may help to verify the present theoretical study.

References

[1] Whitham, G. B., "The Flow Pattern of a Supersonic Projectile," *Communication on Pure and Applied Mathematics*, Vol. 5, 1952, pp. 301–348.

[2] Hayes, W. D., *Linearized Supersonic Flow*, thesis, 1947, California Inst. of Technology.

[3] Lomax, H., "The Wave Drag of Arbitrary Configurations in Linearized Flows as Determined by Areas and Forces in Oblique Planes," RM A55 A18, 1955, NACA.

[4] Carlson, H. W., "Correlation of Sonic-Boom Theory with Wind-Tunnel and Flight Measurements," TR R-213, Dec. 1964, NASA.

[5] Pan, Y. S., "Application of Whitham's Theory to Sonic Boom in the Mid- or Near-Field," *AIAA Journal*, Vol. 8, No. 11, 1970, pp. 2080–2082.

[6] Morris, O. A., Lamb, M., and Carlson, H. W., "Sonic-Boom Characteristics in the Extreme Near Field of a Complex Airplane Model at Mach Numbers of 1.5, 1.8, and 2.5," TN D-5755, April 1971, NASA.

[7] Ward, G. N., *Linearized Theory of Steady High-Speed Flow*, Cambridge University Press, London, 1955, Chaps. 8 and 9.

[8] Ferri, A. and Schwartz, I. R., "Sonic Boom Generation, Propagation and Minimization," *AIAA Paper* 72-194, San Diego, Calif., 1972.

[9] Siegelman, D., "Pressure Signature of An Axisymmetric Body at Angle of Attack," *AIAA Journal*, Vol. 5, No. 12, 1967, pp. 2280–2281.

[10] Goethert, B. H., *Fundamental Research on Advanced Techniques for Sonic Boom Suppression*, Contract DTO FA 70 WA-2260 Final Report, Federal Aviation Administration, Nov. 1971, Sec. 2.1.

[11] Hayes, W. D. and Probstein, R. F., *Hypersonic Flow Theory*, Vol. 1, Academic Press, New York, 1966, pp. 480–497.

[12] Ferri, A., "The Method of Characteristics," *General Theory of High Speed Aerodynamics*, edited by W. R. Sears, Princeton N. J., 1954, p. 664.

[13] Courant, R. and Friedrichs, K. O., *Supersonic Flow and Shock Waves*, Interscience, N. Y., 1948, Chaps. 3 and 4.

[14] Bauer, R. C., private communication, 1971

[15] Kutler, P. and Lomax, H., "Shock-Capturing, Finite-Difference Approach to Supersonic Flow," *Journal of Spacecraft and Rockets*, Vol. 8, No. 12, 1971, pp. 1175–1181.

[16] Hayes, W. D., "Pseudotransonic Similitude and First-Order Wave Structure," *Journal of the Aerospace Sciences*, Vol. 21, 1954, pp. 721–730.

NOVEMBER 1972 AIAA JOURNAL VOL. 10, NO. 11

Turbulence Structure Parameters in an Inhomogeneous Strain Field

P. A. C. OKWUOBI,* R. S. AZAD,† AND O. HAWALESHKA‡
The University of Manitoba, Winnipeg, Canada

The results of some study of the structure parameters in developed turbulent shear flow in a conical diffuser are presented. Measurements of the structure parameters along the diffuser axis were taken for two flow rates. The results show that along the diffuser axis, the structure parameters remain essentially constant and equal in magnitude to the value at the axis in the fully developed pipe flow. Reynolds number and changes in the total turbulent kinetic energy have a negligible effect on the structure parameters From the study of the equilibrium time scale, it is observed that the turbulence structure tends to quickly adapt itself to the change in the flow condition.

Nomenclature

a_1, a_2, a_3 = constants
D = diameter of inlet pipe
K_1 = $(<v>^2 - <w>^2)/(<v>^2 + <w>^2)$
K_1^* = $(<u_1>^2 - <u_2>^2)/(<u_1>^2 + <u_2>^2)$
K_2^* = $(<u_2>^2/<u_1>^2)^{1/2}$
k_t = hot wire cooling constant
L = length of pipe preceding the diffuser
q^2 = $<u_1>^2 + <u_2>^2 + <u_3>^2$
Re = Reynolds number, $U_m D/\nu$
t = time
U_1, U_2, U_3 = components of mean velocity in the axial, radial and circumferential directions
u_1, u_2, u_3 = components of fluctuating velocity in the axial, radial and circumferential directions
u, v, w = components of fluctuating velocity in Cartesian coordinates
U_{ef} = effective cooling velocity
U_m = cross section average velocity at the diffuser inlet
$U_{\max}$ = center line mean velocity at the diffuser inlet
U_* = friction velocity
U^+ = U_1/U_*
x, r = axial and radial directions
y = radial distance from pipe wall
Y^+ = yU_*/ν
α = total effective strain
β = constant
ε = dissipation rate, $15\nu<u_1>^2/\lambda^2$

Received December 20, 1971; revision received March 20, 1972. The authors wish to thank R. Hummel for his help with the electronics. The financial support of the National Research Council of Canada is gratefully acknowledged.

Index categories: Boundary Layers and Convective Heat Transfer—Turbulent; Subsonic and Transonic Flow.

* Research Fellow, Department of Mechanical Engineering.
† Associate Professor, Department of Mechanical Engineering.
‡ Assistant Professor, Department of Mechanical Engineering.